Mechanistic and kinetic studies on glyoxal oxidation with Bi- and Pb-promoted Pd/C catalysts

F. Alardin, H. Wullens, S. Hermans, M. Devillers*

Unité de Chimie des Matériaux Inorganiques et Organiques, Université Catholique de Louvain, Place Louis Pasteur, 1/3, B-1348 Louvain-La-Neuve, Belgium

Abstract

Bimetallic Pd–M/C catalysts (M = Bi, Pb) for the selective oxidation of glyoxal into glyoxalic acid were prepared either from inorganic salts or from acetate-type precursors. The bimetallic catalysts were found to be very active, confirming the promoting ability of both bismuth and lead in this reaction. The magnitude of their effect in terms of activity and selectivity was similar, and dependent on the preparation method and on the composition (optimum for ratios Pd:M = 1). The heavy elements could play their promoter role when introduced in solution in combination with a monometallic Pd/C catalyst. A kinetic treatment of the complex reaction scheme was carried out, and the rate constants for each step were determined. This showed that the reaction proceeds through a real heterogeneous mechanism involving the catalyst for the oxidation of glyoxal into glyoxalic acid and then, in a second step, into oxalic acid. The direct formation of oxalic acid from glyoxal could be neglected, and the formation of glycolic acid was confirmed to depend only on the pH. The absence of deactivation with our catalysts was also demonstrated. Correlations between the rate constants and some surface characteristics of the promoted catalysts were evidenced.
© 2004 Elsevier B.V. All rights reserved.

Keywords: Pd/C catalysts; Glyoxal oxidation; Bismuth; Lead; Glyoxalic acid

1. Introduction

We have reported recently [1,2] that the use of bimetallic catalysts for the selective oxidation of glyoxal into glyoxalic acid could be highly advantageous. The incorporation of a promoter element such as bismuth or lead onto a Pd/C catalyst leads to improvements both in terms of activity and selectivity when compared to the initial report on the use of heterogeneous catalysts for this reaction [3]. In this early study, the authors recommended the use of monometallic catalysts based on a noble metal (Pt, Pd, Rh, Ir) supported on a carbonaceous support. This type of catalyst is commonly used for the liquid phase oxidation of alcohols and aldehydes to their corresponding acids [4,5], and the promoting ability of post-transition heavy elements (such as bismuth or lead) had already been recognised for other transformations

[6–11]. Selective oxidations represent an important challenge for the valorisation of renewable feedstocks, allowing for example the use of biomass-derived compounds for the production of high added-value chemicals [12].

In this paper, we have taken a kinetic approach to study more in detail the catalytic oxidation of glyoxal, and the action of bimetallic catalysts based on carbon-supported palladium in association with bismuth or lead. A kinetic approach for this reaction is easily justified by the fact that several parallel and consecutive reactions are involved (see Fig. 1), which can also lead to oxalic, formic, and glycolic acids in addition to the desired product, glyoxalic acid. This latter acid is desirable for its uses as an intermediate in the food, fragrance and pharmaceutical industries [13,14]. For example, through a reaction with guaiacol, it can serve as a starting material for the synthesis of vanillin [15–17]. In addition, glyoxalic acid is industrially still produced by using stoichiometric amounts of strong acids [10], rather than via a catalytic process, which would be much more environmen-

* Corresponding author. Tel.: +32 10 472 827; fax: +32 10 472 330.
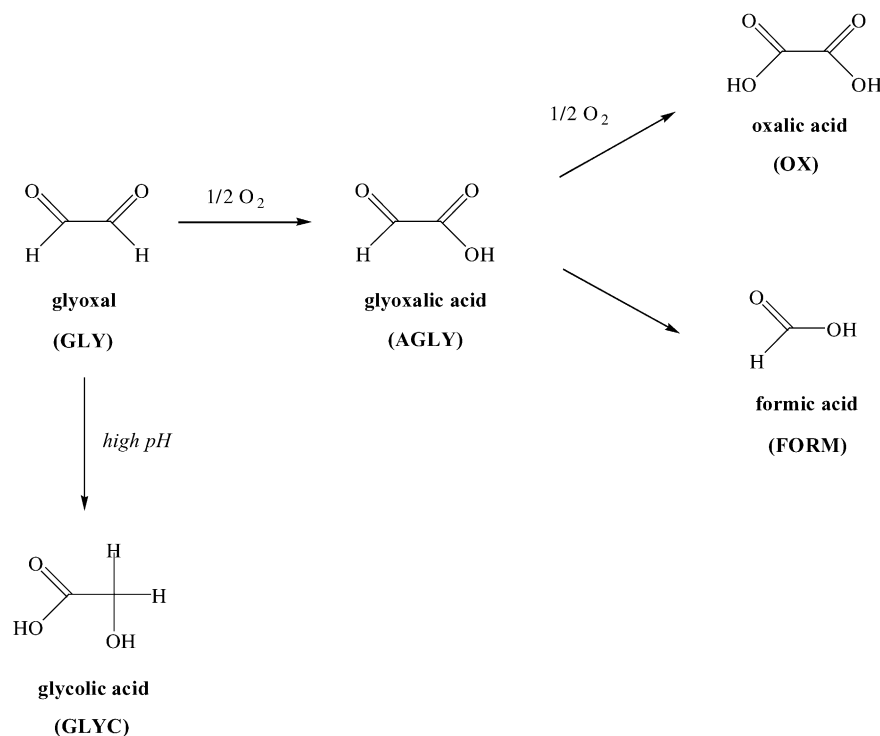*E-mail address:* devillers@chim.ucl.ac.be (M. Devillers).

Fig. 1. Overall reaction scheme for the liquid phase oxidation of glyoxal.

tally friendly. The optimisation and detailed understanding of heterogeneous catalysts for this reaction is thus necessary. Other methods for the synthesis of glyoxalic acid have been proposed in the literature: a chemo-enzymic route starting from glyoxal through glycolic acid, using a glycolate oxidase from spinach [18,19], the electroreduction of oxalic acid [20,21], or the simultaneous anodic oxidation of glyoxal and cathodic reduction of oxalic acid [22,23]. The obvious limitation of these various proposals, when compared to the heterogeneously catalysed one, resides in the industrial upscaling of such enzymatic or electrochemical processes.

2. Experimental

Most materials and methods are very similar to the ones described in our earlier reports [1,2].

2.1. Catalysts synthesis

The support used in all cases is an active carbon from the NORIT firm, called SX+, and characterised by a high surface area ($\sim$1000 m^2/g), from which only the portion with a granulometry comprised between 50 and 100 μm was kept. The total metal loading in bimetallic catalysts was in all cases 10 wt.% (Bi + Pd or Pb + Pd, 5 wt.% in each metal unless otherwise stated), and 5 wt.% in monometallic catalysts. Two types of catalysts were prepared, depending on the type of precursors used: (i) the "reference" catalysts (noted Ref.), prepared according to a patent [24] from inorganic salts

of the metals, i.e. palladium(II) chloride (PdCl$_2$, Janssen), bismuth(III) nitrate pentahydrate (Bi(NO$_3$)$_3\cdot$5H$_2$O, Fluka), or lead(II) nitrate (Pb(NO$_3$)$_2$, Merck); and (ii) the catalysts prepared from acetate-type precursors (noted Ac), which are: palladium(II) acetate (Pd(OAc)$_2$, Acros), bismuth(III) oxoacetate (BiO(O$_2$CCH$_3$), synthesised according to [25]) or lead(II) acetate trihydrate (Pb(O$_2$CCH$_3$)$_2\cdot$3H$_2$O, Acros).

2.1.1. Pd–Pb/C catalysts

The reference catalysts, noted Ref.PbPd/C$_{SX+}$, were prepared according to [24], by using PdCl$_2$ and Pb(NO$_3$)$_2$. In summary, the lead precursor (0.40 g) is dissolved in acidified water (10 ml conc. HCl + 40 ml H$_2$O) and brought into contact with the carbon support (4.5 g) for 6 h under magnetic stirring at ambient temperature, before adding dropwise a solution of the Pd precursor (4.2 ml of a solution which contains 6 wt.% Pd). After addition of NaOH in order to reach a basic pH (40 ml NaOH 20 wt.%), the metals are reduced by formalin (1.2 ml HCHO 37%) at 80 °C (reaction time: 1 h). The catalyst is then recuperated by filtration, washed with water, and dried under vacuum at 30 °C for 3 h. The acetate-type catalysts, noted Ac.PbPd/C$_{SX+}$, were prepared by suspending the palladium precursor (0.53 g Pd(OAc)$_2$) and the carbon support (4.5 g) in heptane (200 ml), followed by sonication for 30 min, and slow evaporation of the solvent under reduced pressure at ambient temperature. This monometallic non-activated catalyst is then reintroduced in suspension in 200 ml heptane with the dehydrated (by heating for 3 h at 100 °C) lead precursor (0.46 g Pb(O$_2$CCH$_3$)$_2$), sonicated for 30 min, and the solvent is re-

moved similarly. This type of catalysts is then activated by heating in a tubular oven for 18 h at 500 °C under a constant nitrogen flow. Obviously, monometallic catalysts can also be prepared following this method, by using a single deposition step with the adequate metallic precursor. These are the noted: Ac.Pd/C$_{SX+}$, Ac.Pb/C$_{SX+}$, or Ac.Bi/C$_{SX+}$. In addition, for the Ac.PbPd/C$_{SX+}$ catalysts, the molar ratio between the two metallic components was varied, by repeating the same synthetic procedure with the adequate amounts of both precursors in order to obtain in the final (activated) catalysts a total metal loading of 10 wt.% but a molar ratio Pb/Pd equal to 2, 1, 0.6 or 0.33. These catalysts are noted Ac.xPbyPd/C$_{SX+}$, where x and y represent the amount in each metal with respect to the other (in moles).

2.1.2. Pd–Bi/C catalysts

Identical procedures were used to prepare reference and acetate-type Pd–Bi/C catalysts, respectively, noted Ref.BiPd/C$_{SX+}$ and Ac.BiPd/C$_{SX+}$. A trimetallic commercial catalyst Pd(4%)–Pt(1%)–Bi(5%)/C from Degussa was also used for comparison purpose.

2.1.3. Pure alloys

Given that intermetallic compounds appear in both Pd–Bi and Pd–Pb phase diagrams [26], their presence might be suspected at the surface of the activated bimetallic catalysts. In order to have a "model" for XRD characterisation and intrinsic catalytic activity, pure (unsupported) alloys were also prepared from the acetate-type precursors. The synthetic procedure involves the sonication of a mixture of the two metallic precursors concerned, in heptane, followed by slow evaporation of the solvent, and thermal treatment in a tubular oven as described above. The intermetallic compound Pd$_3$Pb could be obtained from 2.0198 g palladium acetate and 0.9756 g dehydrated lead acetate, and is noted Ac.Pd$_3$Pb. The synthesis of the unsupported alloys Pb–Pd, Pb$_2$Pd and Pb$_3$Pd$_5$ were attempted following the same method (from the same precursors in different amounts), with adapted degradation temperatures determined from the phase diagram [26], but a mixture of Pd$_3$Pb and PbO or PdO was obtained in all cases. Therefore, these impure phases were not used any further.

2.2. Catalytic tests

The catalytic tests were carried out as before [1,2], using a double-walled glass reactor, with water circulation for thermostatic control, and a mechanical stirrer (Heidolph RZR 2051). The acids formed are neutralised continuously by addition of NaOH in order to keep the pH at a constant value of 7.7. This is done automatically by using the Stat Titrino 718 from Metrohm, together with a combined electrode Beckman 39843. The experimental conditions used routinely for catalysts testing (called the "standard" conditions in this paper) are the following: starting volume of glyoxal solution (0.1 mol/l): 400 ml, temperature: 38 °C, stirring rate: 1000 rpm, pH: 7.7, air flow (oxidant): 0.4 l/min, and mass of catalyst: 100 mg. In addition, when the ratio between the two metals in bimetallic Pb–Pd catalysts was varied, catalytic tests with a constant Pd mass (2 mg Pd in total) were also carried out, by engaging different amounts of catalyst (33–100 mg), depending on its composition.

The products formed were quantified by HPLC (liquid chromatograph TSP Spectra Series P200), on an Aminex Bio-Rad HPX-87H column, heated at 60 °C, and using sulphuric acid (solution 0.005 mol/l) as eluent (flow rate: 0.4 ml/min). The products are detected at 230 nm on a TSP Spectra System UV6000LP diode array detector, and the quantification is possible after calibration with standard solutions. The reaction mixtures were also analysed by atomic absorption (after removal of the catalyst by filtration), using a Perkin-Elmer 3110 spectrometer, in order to detect metal leaching (if any).

The catalytic results are expressed in terms of yield in each acid (Y, %; see Fig. 1 for abbreviations used for reaction products), conversion (X, %) and selectivity (S, %), defined as follows (*Note*: formic acid has been neglected in the remainder of this paper, because its mean yield never exceeds 3% after 24 h with bimetallic Pd–Pb/C or Pd–Bi/C catalysts [1]):

$$Y = \frac{C_{product}}{C_{glyoxal\ at\ t=0}} \qquad C = \text{concentration} \tag{1}$$

$$X_{GLY} = Y_{AGLY} + Y_{OX} + Y_{GLYC} \tag{2}$$

$$S_{AGLY} = \frac{Y_{AGLY}}{X_{GLY}} \tag{3}$$

When the yield in glycolic acid is neglected (because its formation does not depend on the catalyst but only on the pH), a "corrected" conversion (X^*, %) and a "corrected" selectivity (S^*, %) are quoted, following:

$$X^*_{GLY} = Y_{AGLY} + Y_{OX} \tag{4}$$

$$S^*_{AGLY} = \frac{Y_{AGLY}}{X^*_{GLY}} \tag{5}$$

2.3. Physico-chemical methods of characterisation

Photoelectron spectroscopy (XPS) was carried out on a Surface Science Instruments SSI-100 spectrometer (type 206) from Fisons, coupled with a Hewlett-Packard 9000/310 computer. The photopeaks considered for quantification are C 1s, Pd 3d, Pb 4f, and Bi 4f. The energy scale is corrected by using a theoretical value of 284.8 eV for the C 1s peak (C–C, H). The powder X-ray diffraction (XRD) analyses were carried out on a Siemens D-5000 diffractometer, equipped with a Cu source ($\lambda_{K\alpha}$ = 154.18 pm). The samples were supported on quartz monocrystals (supplied by Siemens), and the crystalline phases were identified with reference to the JCPDS database. The thermogravimetric analyses (TGA) were performed on a Setaram TGC 85 analyser, coupled with a Setaram calorimeter (type 1142) and a Hewlett-Packard 86B computer.

3. Results and discussion

3.1. Catalysts preparation

As described in more details in the experimental part, various mono- or bimetallic Pd–M/C catalysts (M = Pb or Bi) were prepared via two distinct routes: either following a method described in a patent [24] starting from inorganic salts, to give what we call "reference" catalysts (noted Ref), or by deposition in heptane starting from acetate-type complexes (the catalysts in this case are noted Ac). Given that the catalysts prepared by this latter route are activated thermally, the behaviour of the acetate-type precursors upon heating under nitrogen was studied independently by TGA between 20 and 500 °C (heating ramp: 10 °C/min). Moreover, the residues of TGA analyses were characterised by XRD in order to determine their nature. It was found that: (i) palladium acetate is transformed totally into Pd metal above 260 °C; (ii) lead acetate is decomposed into a mixture of Pb metal and PbO above 400 °C; and (iii) bismuth oxoacetate leads to mainly Bi_2O_3 above 380 °C. When a mixture of palladium acetate and lead acetate (in a Pb/Pd 1/1 wt. ratio) is heated in the TGA apparatus, the decomposition pattern in slightly different than with each precursor taken separately, because the weight loss (40.3% at 400 °C, before reaching a plateau) corresponds to the formation of both metals. When analysing the residue by XRD, both Pd_3Pb and Pd_5Pb_3 alloys were detected, in accord with the binary Pb–Pd phase diagram [26]. Similarly, the formation of Bi–Pd alloys by heating mixtures of palladium acetate and bismuth oxoacetate had already been documented by us within the framework of the glucose oxidation reaction [27].

3.2. Catalysts characterisation

The results of characterisation by XRD and XPS of the activated Pd–M/C catalysts (M = Bi, Pb) have already been reported partially elsewhere [1,2]. The phases detected by XRD for the various mono- and bimetallic catalysts described in this paper are summarised in Table 1. It is interesting to note that in all the bimetallic catalysts Ac.xPbyPd/C_{SX+}, with variable composition, the only alloy detected in all cases was Pd_3Pb. No major change was observed for any of the catalysts after use in glyoxal oxidation. The results of XPS characterisation tend to suggest that: (i) the metals are relatively well dispersed on the support in all cases, because the experimental Pb/C, Pd/C and Bi/C atomic ratios are systematically higher than the theoretical values calculated on the basis of the bulk composition; (ii) the heavy elements cover at least partially the palladium in the bimetallic catalysts, as the Bi/Pd and Pb/Pd atomic ratios are also higher than the calculated values; and (iii) the Bi/C and Pb/C ratios are lower after test, in line with the leaching behaviour of these two elements during catalyst use [2]. With the Ac.xPbyPd/C_{SX+} catalysts, where the composition was varied, these trends are not as clear, as the amount of surface Pb found even before test (but after

Table 1
Phases detected by XRD in the activated catalysts (before test)

Catalyst	Phases identified
Monometallic catalysts	
Ac.Pd/C_{SX+}	Pd
Ac.Bi/C_{SX+}	Bi, Bi_2O_3
Ac.Pb/C_{SX+}	Pb, PbO
Bimetallic catalysts with M/Pd = 1	
Ac.PdBi/C_{SX+}	Bi_xPd_y
Ref.PdBi/C_{SX+}	Pd
Ac.PbPd/C_{SX+}	Pd_3Pb
Ref.PbPd/C_{SX+}	Pd_3Pb
Bimetallic catalysts Ac.xPbyPd/C_{SX+}	
Ac.2Pb1Pd/C_{SX+}	Pd_3Pb
Ac.3Pb5Pd/C_{SX+}	Pd_3Pb, Pd
Ac.1Pb3Pd/C_{SX+}	Pd_3Pb (+Pd?)
Commercial catalyst	
Pd–Pt–Bi/C (Degussa)	$Bi_2O_2CO_3$, Pd

activation) is lower than expected. This remains to be fully explained, but might be related to the presence of the Pd_3Pb alloy in all these Ac.xPbyPd/C_{SX+} catalysts.

3.3. Optimisation of the catalytic testing procedure

In order to be able to conduct kinetic studies, one has to be certain that the catalyst's activity is not limited by diffusion phenomena. A few preliminary steps were thus conducted on the catalytic testing parameters, in order to ensure optimal testing conditions.

First, the influence of the pH was studied. It was found that, in the absence of any catalyst, when the pH is increased, the production of the undesirable by-product glycolic acid increases exponentially (Y_{GLYC} = 65.5% after 2 h reaction time at pH 9.5). This is due to the fact that glycolic acid is produced by Cannizzaro dismutation in the presence of a base. In order to avoid its formation, an acid pH would be preferred, but this is a drawback for the activity, as it favours the formation of oligomeric forms of glyoxal that are less reactive. A good compromise was found in fixing the pH at a value of 7.7. In the presence of a catalyst or the carbon support alone, the production of glycolic acid follows the same trends, showing its dependency only on the pH. When the reaction duration is increased, the amount of glycolic acid produced increases linearly, regardless of the nature (or even presence) of the catalyst. These experiments justify the use of "corrected" conversion and selectivity, as we define them (see Section 2, Eqs. (4) and (5)), to characterise the catalysts activity.

Second, the absence of diffusional limitation was verified by several different manners. Firstly, the stirring rate was varied between 1000 and 1800 rpm, keeping all other testing parameters constant, and using a "reference" Bi–Pd/C catalyst. It was found that the conversion and yields obtained were identical in all cases. Secondly, the air flow was varied between 0.4 and 1.0 l/min. Again, the results obtained (keep-

ing all other parameters constant) with the reference catalyst were always the same. Thirdly, the mass of catalyst was varied between 0 and 350 mg, and the corrected conversion (to evaluate only the effect of the catalyst itself by neglecting the Cannizzaro dismutation which depends only on the pH) was found to increase linearly with respect to the mass of catalyst until the value of 300 mg. Above this limit, a kinetic regime could not be ensured anymore, as the conversion becomes limited by diffusional problems. Finally, two Ac.BiPd/C$_{SX+}$ catalysts were prepared on different fractions of SX+ carbon with different particle sizes: 50–100 and 100–200 μm. The catalytic activity of these two catalysts was very similar (at reaction times = 2, 4 or 20 h), confirming the absence of internal diffusional limitation in this range. All these experiments confirmed that the "standard" testing conditions chosen (using 100 mg of catalyst, a stirring rate of 1000 rpm and an air flow of 0.4 l/min, see Section 2) are adequate for a kinetic study.

Finally, the necessity of a supported metal catalyst for the formation of the oxidation products (glyoxalic and oxalic acids) was also verified, by conducting catalytic tests in the absence of any catalyst or in the presence of the support alone. The yields in glyoxalic and oxalic acids were in both cases equal to zero. Similarly, when tests are carried out without catalyst or with the support alone, but starting with either glyoxalic, oxalic or glycolic acids rather than glyoxal as reactant, the yields in any of the other acids stay unsignificant. This means that the possibility of a homogeneous intermolecular Cannizzaro reaction (which would produce 1 mol of oxalic acid and 1 mol of glycolic acid from 2 mol of glyoxalic acid) can be discarded.

3.4. Catalytic results

3.4.1. Comparison between Pb- and Bi-promoted catalysts

The mono- and bimetallic catalysts prepared by the two different methods were tested in standard conditions for glyoxal oxidation. In order to obtain a graph for the evolution of the yields in different products as a function of time, and to allow the kinetic studies – which will be presented in the next section – to be carried out, catalytic tests of variable duration were performed, ranging from 30 min to 30 h. Fig. 2 shows a comparison of the yields in glyoxalic acid obtained with the various catalysts prepared via the acetate route (i.e. by dispersion in heptane and thermal activation) [2]. It is obvious from this graph that both lead and bismuth can play a significant promoter role for this reaction. Indeed, the three Pd/C, Bi/C and Pb/C monometallic catalysts present very little or no activity (even for prolonged period of time), while both bimetallic Pd–Bi/C and Pd–Pb/C catalysts are very active. It seems however that the promoting ability of bismuth is higher than that of lead, as the maximum yield in glyoxalic acid obtained with the Ac.BiPd/C$_{SX+}$ catalyst is 15.2% (after 24 h), while it is only 10.5% after 24 h for the Ac.PbPd/C$_{SX+}$ material. The inverse trend is observed for the catalysts pre-
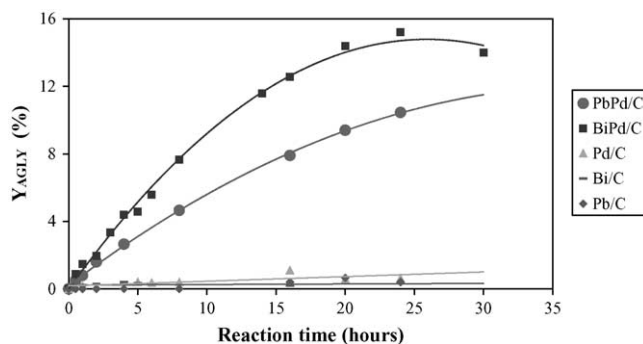

Fig. 2. Yield in glyoxalic acid as a function of time for the various catalysts prepared from acetate-type precursors [2].

pared following the patent's method [24]: the maximum yield in glyoxalic acid obtained with the Ref.BiPd/C$_{SX+}$ catalyst is 9.3% (after 16 h), while it is 13.6% (after 20 h) for the Ref.PbPd/C$_{SX+}$ catalyst (and the corrected conversion for this latter catalyst is always higher than for the former). These two "reference" catalysts display very similar selectivities. On the contrary, the Ac.PbPd/C$_{SX+}$ is more selective than the Ac.BiPd/C$_{SX+}$ catalyst, even if the corrected conversion for Ac.PbPd/C$_{SX+}$ is lower than for Ac.BiPd/C$_{SX+}$. With the trimetallic Pd(4%)–Pt(1%)–Bi(5%)/C Degussa catalyst, the maximum yield in glyoxalic acid is reached after 8 h of reaction, but is only 9.8%. We have thus succeeded in preparing performant catalysts for the oxidation of glyoxal. In all cases, after the maximum yield in glyoxalic acid is reached, the selectivity drops because the yield in oxalic acid increases: this is the onset of the second step in the consecutive oxidation reactions (see Fig. 1) and can be called over-oxidation.

When considering in more details the performance of Pd–Pb/C catalysts, it is interesting to compare the performance of the catalysts prepared via the two different methods and using different precursors, namely Ref.PbPd/C$_{SX+}$ (prepared by the patent method) and Ac.PbPd/C$_{SX+}$ (prepared via the acetate route). This is presented in Fig. 3. As mentioned above, the Ref.PbPd/C$_{SX+}$ catalyst is more active, which can be seen by comparing the conversion (Fig. 3(a)). However, this same Ref.PbPd/C$_{SX+}$ catalyst is less selective than its Ac.PbPd/C$_{SX+}$ counterpart, as Fig. 3(b) shows clearly by comparing their corrected selectivities S^*. The corrected selectivity for the Ac.PbPd/C$_{SX+}$ catalyst stays high (above 65%) over long periods of time (up to 24 h), while it is only 32% after 24 h for the Ref.PbPd/C$_{SX+}$ catalyst.

When considering the phase diagram for the bimetallic association Pd–Pb [26], the presence of intermetallic Pd$_x$Pb$_y$ compounds might be suspected at the surface of the catalysts prepared by the acetate route. Indeed, with a global composition of Pb/Pd = 0.51, and a thermal activation at 500 °C, both Pd$_3$Pb and Pd$_5$Pb$_3$ might form in the Pd(5 wt.%)–Pb(5 wt.%)/C catalysts. When the carboxylate precursors (in a wt. ratio 1/1) are mixed in a pure form (without support) and heated at 500 °C, an analysis by XRD of the
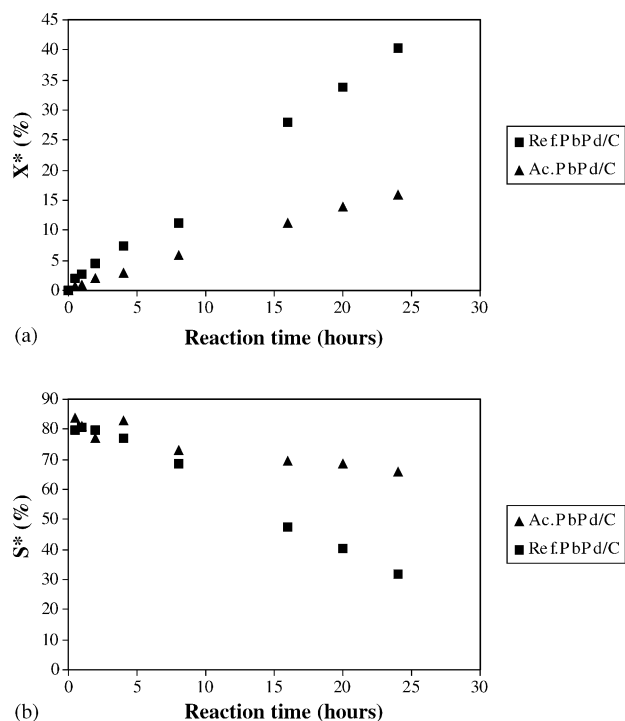
Fig. 3. Comparison of the Ref.PbPd/C$_{SX+}$ and the Ac.PbPd/C$_{SX+}$ catalysts, in terms of (a) "corrected" conversion and (b) "corrected" selectivity.
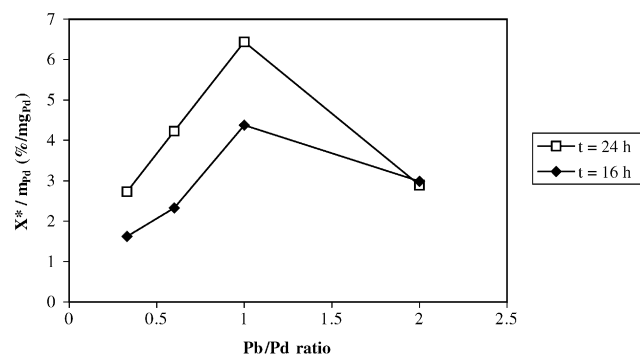

Fig. 4. Corrected conversion (normalised with respect to the Pd mass) in function of the Pb/Pd molar ratio for the catalysts Ac.xPbyPd/C$_{SX+}$ characterised by a variable composition, for a total metal loading (Pb + Pd) of 10 wt.%, and using 100 mg of catalyst in each test.

residue has revealed the presence of both alloys (see above). In the real (supported) catalysts, only Pd$_3$Pb was detected (see Table 1). This tends to suggest that another Pb-rich phase (maybe PbO) is present on the surface of the support, in an amorphous state. The pure alloy Ac.Pd$_3$Pb was prepared intentionally (see Section 2), and tested in glyoxal oxidation. Its purity was first verified by XRD, and then 50 mg were used in standard testing conditions. The conversion obtained with this Ac.Pd$_3$Pb material is low ($X^* < 3\%$ at $t = 20$ h), but this is due to the low surface area (16 m^2/g) of this unsupported phase. Interestingly, the evolution in time of the yields in glyoxalic and oxalic acids, as well as the selectivity, obtained with the Ac.Pd$_3$Pb alloy, were very similar to those obtained with the Ac.PbPd/C$_{SX+}$ catalyst. The lead leaching in the reaction medium from the Ac.Pd$_3$Pb alloy over time was measured, and was found to stay under 6% at all times. This might be explained by the stability of such alloys, as was also observed for Pd$_3$Bi [27]. The Ac.Pd$_3$Pb alloy was also characterised by XPS, in order to gain information on its surface composition, and it was found that the surface is enriched in lead, in accord with the relative surface free energies of both metals [28]. The syntheses of the other possible Pb–Pd alloys (PbPd, Pb$_2$Pd, Pb$_3$Pd$_5$ and PbPd$_3$) were also attempted, but a mixture of Pd$_3$Pb and PbO or PdO was obtained in all cases. This is in accord with the Pb–Pd supported catalysts, where the phase Pd$_3$Pb is the only alloy detected, regardless of the composition (see above, results of XRD characterisation). These bimetallic catalysts Ac.xPbyPd/C$_{SX+}$, with variable composition, were also tested for glyoxal oxidation, and

it was found that the activity is affected by the Pb/Pd ratio in the catalysts. Fig. 4 shows the corrected conversion X^* (normalised with respect to the Pd mass) as a function of the Pb/Pd ratio. It is obvious from this figure that an optimum in terms of activity is obtained for the catalyst characterised by a ratio Pb/Pd = 1, which parallels exactly the results obtained with Bi–Pd/C catalysts [1]. The same evolution is observed when considering only the yield in glyoxalic acid rather than the global conversion. However, when considering the corrected selectivity S^*, the order is slightly different, with an optimum ($S^* \geq 90\%$) corresponding to the composition Pb/Pd = 0.6, when carrying out the catalytic tests with a mass of catalyst of 100 mg regardless of the composition. When the catalytic tests were carried out in such a way that the total Pd mass engaged was constant (by varying the amount of catalyst used in each test as a function of its composition), the selectivity was found to vary only little, and to stay very high ($\approx 90\%$). The best compromise in terms of *both* activity and selectivity for the Ac.xPbyPd/C$_{SX+}$ catalysts corresponds to a molar ratio Pb/Pd = 0.5, i.e. a wt. ratio of 1/1, as in the "reference" catalyst. After 24 h reaction time, the Pb leaching from the various Ac.xPbyPd/C$_{SX+}$ catalysts was found to be maximum 25% of the amount of Pb initially present in the catalyst. This is very similar to the amount of Bi leaching detected with equivalent Bi–Pd/C catalysts for the same reaction [1]. A more detailed analysis of the stability of these promoted catalysts in this reaction has been reported elsewhere [2].

### 3.4.2. Role of the solubilised promoter in the catalytic activity

Given the occurrence of leaching of the promoter element (Bi or Pb) in the reaction mixture (although much more limited than in the case of glucose oxidation) [2], catalytic tests were performed using the standard conditions, without catalyst, but in the presence of either lead or palladium in solution (respectively, Pb^{2+} at a concentration of 2.4×10^{-5} mol/l and Pd^{2+} at a concentration of 4.7×10^{-5} mol/l). In all cases, for

reactions times ranging from 2 to 24 h, no oxidation product (glyoxalic or oxalic acid) was detected at the end of the test. A heterogeneous catalyst is thus necessary for the reaction. In addition, catalytic tests were carried out with the monometallic Ac.Pd/C_{SX+} catalyst, using the "standard" testing conditions, in the presence of a known amount of solubilised bismuth (arising from a monometallic Ac.Bi/C_{SX+} catalyst brought into contact with the reaction mixture in a preliminary step, and quantified by atomic absorption). A series of experiments were carried out in this fashion, starting from different amounts of Ac.Bi/C_{SX+} catalyst, and, in all cases, the amount of solubilised Bi was on average 5.4 × 10^{-4} mmol, corresponding to a ratio (dissolved Bi/Pd in catalyst) $\cong 1.15 \times 10^{-2}$. It was found that the performances were superior to those of Pd/C alone, indicating that Bi could play its promoter role: after 4 h reaction, the yield in glyoxalic acid was ~5%, in comparison with 0.6% in the presence of the monometallic Pd/C catalyst alone. Moreover, the selectivity was about 40–50%, when it is only 17% without Bi. In order to determine whether Bi was playing its promoter role in its soluble form, or after re-deposition onto the Pd/C catalyst, the carbon-supported material was characterised by XPS after test. Some amount of bismuth was indeed found on the surface of the tested Pd/C catalysts (atomic ratios Bi/C = 0.04–0.09% and Bi/Pd ratios = 0.05–0.07), confirming that the soluble Bi(III) is reduced in situ into (supported) metallic Bi. When equivalent experiments were carried out for Pb, similar results were obtained (Y_{AGLY} = 5.4% after 4 h for the catalyst Ac.Pd/C_{SX+} used in the presence of solubilised lead). These values of about 5% for Y_{AGLY} after 4 h reaction time are very similar to the values obtained with the bimetallic Pd–Bi,Pb/C "reference" catalysts for the same duration of catalytic test.

3.5. Kinetic study

3.5.1. General kinetic analysis

Fig. 1 shows the various products that can be considered when studying glyoxal oxidation. With the catalysts presented in this paper, the formation of formic acid can be neglected. Moreover, the transformation of glyoxalic acid into glycolic + oxalic acids by intermolecular Cannizzaro dismutation can also be discarded (see Section 3.3). This gives rise to the following reaction scheme, and the definition of several rate constants:
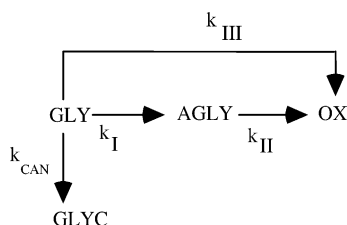
In a first analysis, the direct production of oxalic acid from glyoxal is neglected (k_{III} = 0). Two main processes are thus
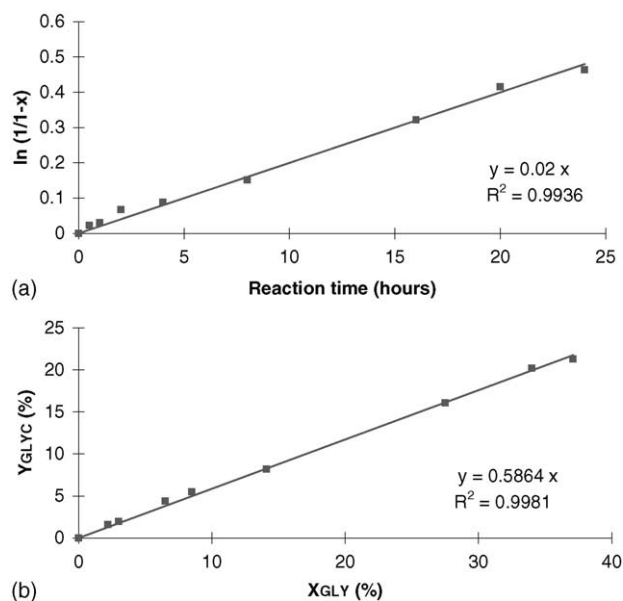

Fig. 5. General kinetics for the catalyst Ac.PbPd/C_{SX+}: (a) evolution of ln(1/1 − x) as a function of time and (b) yield in glycolic acid as a function of glyoxal conversion.

considered for the conversion of glyoxal: (i) the formation of glycolic acid in the homogeneous phase by intramolecular Cannizzaro dismutation; and (ii) the formation of glyoxalic and oxalic acids, which require a heterogeneous catalyst. The rate constant k_{CAN} depends on the pH, which is fixed at a value of 7.7 in our case. It actually represents a pseudo-first-order constant corresponding to $k' \cdot [OH^-]$. The rate constant k_I depends on the partial pressure in oxygen (pO_2) and on the catalyst mass. A first-order kinetics with respect to glyoxal was obtained when plotting the values of ln(1/1 − x) as a function of reaction time for the different catalysts presented in this paper. The slope of the linear plot obtained gives the value of k_{exp}, according to the following equations:

$$v = -\frac{dC_{GLY}}{dt} = k_{CAN} \cdot C_{GLY} + k_I \cdot C_{GLY} = k_{exp} \cdot C_{GLY}$$

with $k_{exp} = k_{CAN} + k_I \Rightarrow k_{exp} \cdot t = \ln\left(\frac{a}{a-x}\right)$

with $a = C_{GLY}$ at $t = 0$ and $a - x = C_{GLY}$ at $t \neq 0$.

When taking $a = 1$, $x = X_{GLY}/100$.

A representative graph for the catalyst Ac.PbPd/C_{SX+} is given in Fig. 5(a). These plots allow us also to confirm the absence of deactivation with all bimetallic catalysts. Only the trimetallic commercial catalyst seems to have a different behaviour, with a rate constant that is high for reaction times inferior to 8 h, but which diminishes afterwards. This indicates that a deactivation phenomenon occurs with this particular catalyst. In order to determine k_{CAN} and k_I, the yields in glycolic acid were plotted against the glyoxal conversion, as shown for a representative catalyst in Fig. 5(b). The slopes of these linear plots give the

Table 2
Values of first-order rate constants (h^{-1}) obtained for the various catalysts described in this paper

	Catalyst				
	Ref.BiPd/C_{SX+}	Ac.BiPd/C_{SX+}	Ref.PbPd/C_{SX+}	Ac.PbPd/C_{SX+}	Pd–Pt–Bi/C (Degussa)
With $k_{III} = 0$ ($k_{exp} = k_{CAN} + k_I$)					
k_{exp}	0.025	0.026	0.039	0.020	0.042
k_{CAN}/k_{exp}	0.391	0.335	0.361	0.586	0.288
k_{CAN}	0.010	0.009	0.014	0.012	0.012
k_I	0.015	0.017	0.025	0.008	0.030
With $k_{III} \neq 0$ ($k_{exp} = k_{CAN} + k_I + k_{III}$)					
k_I/k_{II}	0.132	0.310	0.270	0.310	0.230
k_{III}/k_I	0.020	0.150	0.140	0.120	0.250
k_I	0.0146	0.015	0.022	0.0071	0.024
k_{II}	0.111	0.048	0.081	0.023	0.104
k_{III}	0.0003	0.002	0.003	0.0009	0.006

value of $k_{CAN}/(k_{CAN} + k_I)$. This was determined from the following equations:

$$\frac{dC_{GLYC}}{dt} = k_{CAN} \cdot C_{GLY},$$

$$-\frac{dC_{GLY}}{dt} = (k_{CAN} + k_I) \cdot C_{GLY},$$

$$\frac{dC_{GLYC}}{-dC_{GLY}} = \frac{k_{CAN}}{k_{CAN} + k_I},$$

$$Y_{GLYC} = \frac{k_{CAN}}{k_{CAN} + k_I} \cdot X_{GLY}$$

From the values of rate constants listed in Table 2, it can be seen that the values of k_{CAN} obtained are all very similar (mean value: $(11.3 \pm 2.1) \times 10^{-3}\,h^{-1}$), confirming that the production of glycolic acid is independent of the catalyst. By contrast, the values of k_I are different for each catalyst, with some values being nearly four times higher than others, which shows how sensitive the reaction rate is to the nature of the catalyst.

3.5.2. Detailed mechanistic studies

A more comprehensive data treatment can be carried out in order to determine the other rate constants involved in the overall reaction scheme presented in Section 3.5.1, according to various hypotheses. When assuming in a first step that $k_{III} = 0$, the following equations – based on first-order reactions – can be written:

$$\frac{-dC_{GLY}}{dt} = (k_I + k_{CAN}) \cdot C_{GLY}, \quad C_{GLY} = a\,e^{-(k_I + k_{CAN}) \cdot t}$$

with $a = C_{GLY}$ at $t = 0$,

$$\frac{dC_{AGLY}}{dt} = k_I \cdot C_{GLY} - k_{II} \cdot C_{AGLY}$$

with $C_{GLY} = 1 - x$ and $C_{AGLY} = \frac{Y_{AGLY}}{100}$.

The selectivity towards glyoxalic acid can be deduced from the equation:

$$\frac{dC_{AGLY}}{dC_{GLY}} = \frac{k_I \cdot C_{GLY} - k_{II} \cdot C_{AGLY}}{-(k_I + k_{CAN}) \cdot C_{GLY}},$$

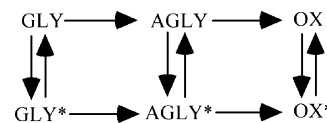$$\frac{dC_{AGLY}}{dC_{GLY}} = \frac{C_{AGLY} - r \cdot C_{GLY}}{r' \cdot C_{GLY}}$$

When defining the following ratios of rate constants:

$$r = \frac{k_I}{k_{II}} \quad \text{and} \quad r' = \frac{k_I + k_{CAN}}{k_{II}} = r\left(1 + \frac{k_{CAN}}{k_I}\right)$$

the differential equation written above can be solved into the following expression, relating the concentration of glyoxalic acid to that of glyoxal:

$$\frac{C_{AGLY}}{a} = \frac{r}{r' - 1} \cdot \left[\left(\frac{C_{GLY}}{a}\right)^{1/r'} - \left(\frac{C_{GLY}}{a}\right)\right]$$

From this, the approach followed consists in plotting C_{AGLY} ($Y_{AGLY}/100$) as a function of C_{GLY} for different values of r chosen for each catalyst. Theoretical curves were obtained by calculating C_{AGLY} (named **v** for clarity) from the values of C_{GLY} (named **u**), where $\mathbf{u} = 1 - x$, and with theoretical values of r. The dotted line refers to a value of $r = 1000$. This is shown in Fig. 6(a) for a representative catalyst. The commercial trimetallic catalyst from Degussa was the only one to display a more complicated behaviour, which is shown in Fig. 6(b). In general, the experimental points that are close to the dotted line correspond to the maximum possible amount of glyoxalic acid produced. The fact that the experimental points are moving away from this dotted line shows that the selectivity in glyoxalic acid is lowering with time. The dotted line is not superimposable to the black (plain) line, because of the simultaneous formation of glycolic acid. The gap between the plain and dotted lines is thus related to k_{CAN}. We have used a least-square iteration method to try to get the best fit between a theoretical curve (arising from a given value of r) and the experimental points. For example, as shown in Fig. 6(a), the best fit was obtained for $r = 0.27$ for the Ac.BiPd/C_{SX+}
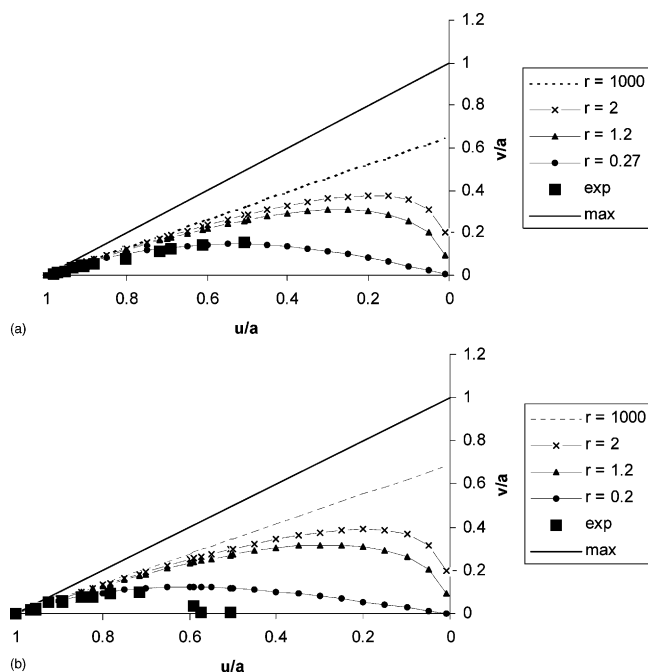
Fig. 6. Detailed mechanistic studies with $k_{III} = 0$: yield in glyoxalic acid (C_{AGLY}) as a function of the amount of glyoxal in solution (C_{GLY}) for different values of r chosen for (a) the catalyst Ac.BiPd/C_{SX+}, and (b) the commercial (trimetallic) catalyst from Degussa (symbols: $a = (C_{GLY})_0$, $u = (C_{GLY})_t$, $v = (C_{AGLY})_t$).

catalyst. However, the fit obtained in all cases was mediocre, suggesting that the simplified reaction scheme based on $k_{III} = 0$ is not appropriate to describe fully the mechanism of the catalysed process.

Therefore, a new reaction scheme was considered, with the possibility of k_{III} being different from zero, i.e. the possibility that oxalic acid would be produced directly from adsorbed glyoxalic acid before its desorption from the catalyst surface, according to the following scheme, in which the asterisk refers to adsorbed species on the surface:
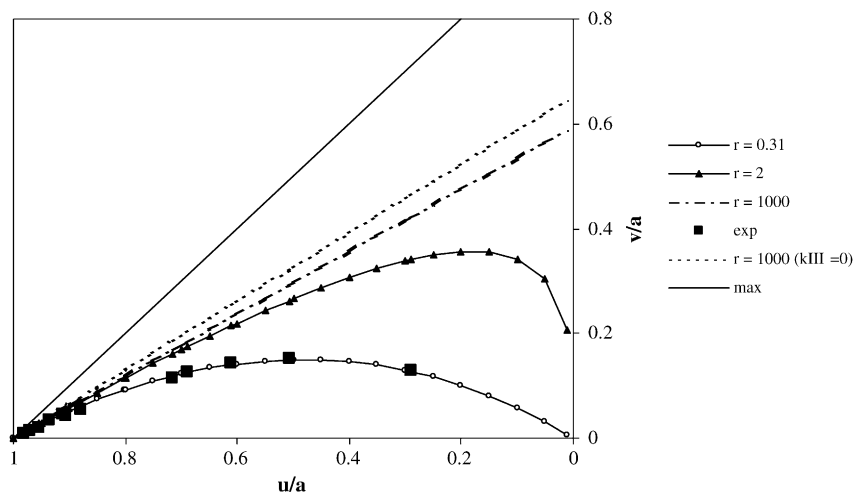
$$GLY \longrightarrow AGLY \longrightarrow OX$$
$$\downarrow\uparrow \qquad \downarrow \qquad \downarrow$$
$$GLY^* \longrightarrow AGLY^* \longrightarrow OX^*$$

The constants k_I, k_{II} and k_{III} correspond thus, respectively, to the transformation of glyoxal into glyoxalic acid (k_I), glyoxalic acid into oxalic acid (k_{II}) and glyoxal into oxalic acid in one step (k_{III}). This gives rise to a new set of equations, as follows:

Taking

$$k_{exp} = k_{CAN} + k_I + k_{III}$$

$$\text{and} \quad r'' = \frac{k_I + k_{CAN} + k_{III}}{k_{II}} = r \left(1 + \frac{k_{CAN} + k_{III}}{k_I} \right),$$

the initial kinetic equations:

$$-\frac{dC_{GLY}}{dt} = (k_I + k_{CAN} + k_{III}) \cdot C_{GLY}$$

$$\text{and} \quad \frac{dC_{AGLY}}{dt} = k_I \cdot C_{GLY} - k_{II} \cdot C_{AGLY}$$

can be transformed into:

$$\frac{dC_{AGLY}}{dC_{GLY}} = \frac{k_I \cdot C_{GLY} - k_{II} \cdot C_{AGLY}}{-(k_{CAN} + k_I + k_{III}) \cdot C_{GLY}}$$

$$= \frac{C_{AGLY} - (r \cdot C_{GLY})}{r'' \cdot C_{GLY}}$$

In the same way as above, solving this differential equation leads to:

$$\frac{C_{AGLY}}{a} = \frac{r}{r'' - 1} \cdot \left[\left(\frac{C_{GLY}}{a} \right)^{1/r''} - \left(\frac{C_{GLY}}{a} \right) \right]$$

with $a = C_{GLY}$ at $t = 0$.

A new set of graphs for each catalyst is thus produced, again by plotting the yields in glyoxalic acid in function of the

Fig. 7. Yield in glyoxalic acid (C_{AGLY}) as a function of the amount of glyoxal in solution (C_{GLY}) for different values of r chosen for the catalyst Ac.BiPd/C_{SX+}, when k_{III} is considered non-equal to zero (symbols: $a = (C_{GLY})_0$, $u = (C_{GLY})_t$, $v = (C_{AGLY})_t$).

Table 3
Correlation between the values of rate constants determined via the kinetic studies and data from XPS characterisation (when values are quoted for tested catalysts, it corresponds to a reaction of 24 h, M = Bi, Pb

XPS	k_{exp} or k_I								
	Degussa	>	Ref.PbPd/C$_{SX+}$	>	Ac.BiPd/C$_{SX+}$	>	Ref.BiPd/C$_{SX+}$	>	Ac.PbPd/C$_{SX+}$
M/Pd									
Fresh	2.29		0.78		0.77		3.77		0.79
Tested	1.42		0.49		0.49		1.59		0.54
Pd/C (×100)									
Fresh	1.11		1.78		1.24		0.97		0.67
Tested	1.10		2.10		1.27		1.51		0.90
M/C (×100)									
Fresh	2.55		1.39		0.95		3.60		0.53
Tested	1.56		1.04		0.62		2.40		0.49
	k_{II}								
	Ref.BiPd/C$_{SX+}$	>	Degussa	>	Ref.PbPd/C$_{SX+}$	>	Ac.BiPd/C$_{SX+}$	>	Ac.PbPd/C$_{SX+}$
M/Pd	3.77		2.29		0.78		0.77		0.79
Pd/C	0.97		1.11		1.78		1.24		0.67
M/C (×100)	3.60		2.55		1.39		0.95		0.53

amount of glyoxal in solution for different values of r, but this time with k_{III} being different from zero. Fig. 7 shows one of these graphs for the same catalyst as before. Again, the dotted line was obtained for $k_{III} = 0$ and $r = 1000$. The new line (-·--·) was obtained by taking k_{III} different from zero and an r value of 1000. The difference between these two lines is attributable to k_{III} itself, the rate constant responsible for the direct transformation of glyoxal into oxalic acid. The difference between the plain line and the dotted line is attributed to k_{CAN}, i.e. to the production of glycolic acid. In all cases, for each different catalyst considered in this study, the best fit obtained between the experimental points and the theoretical curves (for example for $r = 0.31$ in Fig. 7) is better than when k_{III} was considered equal to zero. The final values of rate constants obtained for all catalysts are listed in the lower part of Table 2. The contribution of the direct route from glyoxal to oxalic acid stays quite small, as is shown by the fact that the values of k_{III} obtained are low compared to k_I. In particular, the value of k_{III} for the Ref.BiPd/C$_{SX+}$ catalyst represents only 2% of its value of k_I, while it is between 12 and 15% for the other Pd–M/C catalysts (M = Bi, Pb). By opposition, with the trimetallic catalyst from Degussa, this contribution cannot be neglected anymore, as it represents 25% of the oxidative process consuming glyoxal.

3.6. Discussion

When drawing a parallel between the values of rate constants determined via the kinetic studies and the data from XPS characterisation, some very interesting correlation can be found. In Table 3, the various catalysts have been classified, in the upper part, according to their values of k_{exp} (or k_I), and in the lower part, according to their values of k_{II}. For each catalyst, the values of surface M/Pd, Pd/C and M/C ratios (M = Bi, Pb) determined by XPS have been listed underneath. It is very interesting to note that, if one

excepts the trimetallic Degussa catalyst (which corresponds to a different global composition), a clear correlation exists between the values of k_{exp} (or k_I) and the Pd/C ratios for the home-made catalysts: the glyoxalic acid production is maximised when the palladium dispersion increases. No clear trend exists with regard to the M/Pd or M/C ratios. However, when considering k_{II}, the link with M/C (or M/Pd) is obvious: an increased amount of promoter element present at the surface favours the transformation of glyoxalic into oxalic acid. This probably implies that the promoter element also plays a role in the surface adsorption of glyoxalic acid to allow its further transformation. The values of k_{III} were also compared to the XPS data, but no correlation was found, indicating the occurrence of more complex phenomena for the direct transformation of glyoxal into oxalic acid.

In summary, we have found that the promoter exerts a positive influence on the activity of palladium, which stays very poorly active when used alone. The promoting ability can be conferred through a soluble form of the heavy element, but it is found (in small amounts) on the surface afterwards. The formation of alloys between Pd and the promoter within the catalyst was also demonstrated clearly in the case of Pb. Therefore, the need for an intimate contact between the noble metal and the post-transition element is suspected, with an optimised activity being related to an amount of Pd atoms at the surface that would be maximised, and an optimised selectivity towards glyoxylic acid (i.e. avoiding further oxidation into oxalic acid) being related to a minimised amount of Bi or Pb atoms present at the surface.

4. Conclusion

In this paper, we have shown that lead and bismuth can both act as promoters for the activity of Pd/C catalysts used in glyoxal selective oxidation. The magnitude of their ef-

fects in terms of activity or selectivity is very similar. As was shown before for bismuth, a maximum in terms of yield in glyoxalic acid and "corrected" conversion is attained when the molar ratio between Pd and Pb is close to 1 in the catalyst. In addition, an other parallel can be drawn between Bi and Pb that both leach in solution during catalytic testing (although to a limited extent): when Pd, Pb or Bi alone are used in a soluble form, the oxidation reaction does not take place; however, when the promoter is introduced in solution in combination with a monometallic Pd/C catalyst, the activity reaches the level of bimetallic catalysts, and the promoter element is detected on the surface of the Pd/C material after test. This suggests the occurrence of sophisticated dynamical phenomena at the catalyst's surface during its use.

An extensive kinetic study of the overall reaction scheme has been carried out, and the various rate constants for each step have been determined. It was concluded that the heterogeneously catalysed oxidation proceeds through a consecutive mechanism involving first the formation of glyoxalic acid from glyoxal, and second the formation of oxalic acid from glyoxalic acid in a subsequent step. The direct formation of oxalic acid from glyoxalic acid before its desorption from the catalyst surface could be quantified and shown to be very limited. The confirmation of the origin of glycolic acid in a homogeneous Cannizzaro mechanism, independently of the catalyst, was also obtained. This rearrangement was shown to depend only on the pH, and to be limited to the intramolecular case, while its intermolecular equivalent is negligible. Finally, the absence of deactivation was demonstrated in the case of the "home-made" Pd–M/C catalysts (M = Bi, Pb), in opposition with a commercial trimetallic Pd(4%)–Pt(1%)–Bi(5%)/C catalyst that leads to lowered yields after a very short period of time.

Acknowledgements

References

[1] F. Alardin, P. Ruiz, B. Delmon, M. Devillers, Appl. Catal. A: Gen. 215 (2001) 125.
[2] F. Alardin, B. Delmon, P. Ruiz, M. Devillers, Catal. Today 61 (2000) 255.
[3] P. Gallezot, R. de Mésanstourne, Y. Christidis, G. Mattioda, A. Schouteeten, J. Catal. 133 (1992) 479.
[4] M. Besson, P. Gallezot, Catal. Today 57 (2000) 127.
[5] M. Besson, P. Gallezot, in: R.A. Sheldon, H. van Bekkum (Eds.), Fine Chemicals through Heterogeneous Catalysis, Wiley/VCH, Weinheim, 2001, Chapter 9. p. 491.
[6] H. van Bekkum, Stud. Surf. Sci. Catal. 121 (1998) 117.
[7] M. Wenkin, P. Ruiz, B. Delmon, M. Devillers, J. Mol. Catal. A: Chem. 180 (2002) 141.
[8] T. Mallat, Z. Bodnar, A. Baiker, O. Greis, H. Strübig, A. Reller, J. Catal. 142 (1993) 237.
[9] H. Kimura, A. Kimura, I. Kokubo, T. Wakisaka, Y. Mitsuda, Appl. Catal. A: Gen. 95 (1993) 143.
[10] H. Kimura, K. Tsuto, T. Wakisaka, Y. Kazumi, Y. Inaya, Appl. Catal. A: Gen. 96 (1993) 217.
[11] T. Tsujino, S. Ohigashi, S. Sugiyama, K. Kawashiro, H. Hayashi, J. Mol. Catal. 71 (1992) 25.
[12] B.D. Schutt, B. Serrano, R.L. Cerro, M.A. Abraham, Biomass Bioenergy 22 (2002) 365.
[13] G. Mattioda, Y. Christidis, Ullmann's Encyclopedia of Industrial Chemistry, vol. A12, 5th ed., VCH, Weinheim, 1989, p. 495.
[14] W.J.N. Meester, J.H. van Maarseveen, H.E. Schoemaker, H. Hiemstra, F.P.J.T. Rutjes, Eur. J. Org. Chem. 14 (2003) 2519.
[15] K. Li, J.W. Frost, J. Am. Chem. Soc. 120 (1998) 10545.
[16] M.B. Hocking, J. Chem. Educ. 74 (1997) 1055.
[17] H.R. Bjorsvik, L. Liguori, F. Minisci, Org. Process. Res. Dev. 4 (2000) 534.
[18] G.D. Yadav, V.R. Gupta, Process. Biochem. 36 (2000) 73.
[19] J.E. Gavagan, S.K. Fager, J.E. Seip, D.S. Clark, M.S. Payne, D.L. Anton, R. DiCosimo, J. Org. Chem. 62 (1997) 5419.
[20] J.R. Ochoa, A. Dediego, J. Santaolalla, J. Appl. Electrochem. 23 (1993) 905.
[21] K. Scott, Electrochim. Acta 37 (1992) 1381.
[22] K. Scott, Electrochim. Acta 36 (1991) 1447.
[23] A.F. Jalbout, S.H. Zhang, Acta Chim. Sloven. 49 (2002) 917.
[24] H. Saïto, S. Ohnaka, S. Fukuda, European Patent no. 0142725 B1 (1987).
[25] M. Wenkin, R. Touillaux, P. Ruiz, B. Delmon, M. Devillers, Appl. Catal. A: Gen. 148 (1996) 181.
[26] T.B. Massalski (Ed.), Binary Alloy Phase Diagrams, vol. 1, American Society for Metals, 1986, p. 526;
T.B. Massalski (Ed.), Binary Alloy Phase Diagrams, vol. 2, American Society for Metals, 1986, p. 1834.
[27] M. Wenkin, C. Renard, P. Ruiz, B. Delmon, M. Devillers, Stud. Surf. Sci. Catal. 108 (1997) 391.
[28] A.R. Miedema, Z. Metallk. 69 (1978) 287.